

DMD #4978

**METABOLISM AND DISPOSITION OF A POTENT GROUP II METABOTROPIC GLUTAMATE
RECEPTOR AGONIST, IN RATS, DOGS, AND MONKEYS**

Joyce K. James, Masato Nakamura, Atsuro Nakazato, Kanyin E. Zhang, Merryl Cramer, Janice Brunner,
Jacquelynn Cook, and Weichao G. Chen

Merck Research Laboratories (J.K.J., K.E.Z., M.C., W.G.C.), Merck & Co., Inc., 3535 General Atomics
Court, San Diego, CA 92121

Merck Research Laboratories (J.B., J.C.), Merck & Co., Inc., PO Box 4, Sumneytown Pike, West Point,
PA 19486

Taisho Pharmaceutical Company (M.N., A.N.), LDT, 403 Yoshino – Cho 1 – Chome, Kita-Ku, Saitama –
Shi, Saitama, 331-9530, Japan

DMD #4978

Running Title: Metabolism and Disposition of MGS0028

Correspondence Author: Joyce James
Merck Research Laboratories
Merck & Co., Inc.
3535 General Atomics Court
San Diego, CA 92121-1140
Tel: 858-202-5452
Fax: 858-202-5752
Email: Joyce_James@Merck.com

The number of	Text Pages: 14
	Tables: 5
	Figures: 10
	References: 32
The number of words in the	Abstract: 249
	Introduction: 461
	Discussion: 1360

Abbreviations used are: (H)mGluR ((Human) metabotropic glutamate receptor), CNS (central nervous system), CSF (cerebral spinal fluid), EDTA (ethylene di-amine tetra-acetic acid), HPLC (high performance liquid chromatography), LC-MS (liquid chromatography-mass spectroscopy), PCP (phencyclidine), TLC (thin layer chromatography), DAG (diacylglycerol), IP3 (inorganic phosphate), c-AMP (cyclic adenosine monophosphate), PFB (pentafluorobenzyl bromide)

DMD #4978

Abstract

Metabolism and disposition of MGS0028, a potent group II metabotropic glutamate receptor agonist, were examined in three preclinical species (Sprague-Dawley rats, Beagle dogs, and Rhesus monkeys). In rats, MGS0028 was widely distributed and primarily excreted in urine as parent and a single reductive metabolite, identified as the 4R isomer MGS0034. MGS0028 had a low brain to plasma ratio at efficacious doses in rats and was eliminated more slowly in rat brain than plasma. Exposure increased proportionally (1 -10 mg/kg PO) in rats, with bioavailability >60% at all doses. However, bioavailability was only ~20% in monkeys and MGS0034 was found in relatively high abundance in plasma. In dogs, oral bioavailability was >60% and the metabolite was not detected. *In vitro* metabolism was examined in liver sub-cellular fractions (microsomes and cytosol) from rat, dog, monkey, and human. Reductive metabolism was observed in rat, monkey, and human liver cytosol incubations, but not in dog liver cytosol incubations. No metabolism of MGS0028 was detected in incubations with liver microsomes from any species. Similar to *in vivo* results, MGS0028 was reduced in cytosol stereospecifically to MGS0034. The rank order of *in vitro* metabolite formation (monkey >> rat ~ human >> dog) was in agreement with *in vivo* observations, in rats, dogs, and monkeys. Based on the observation of species difference in reductive metabolism, rat and monkey were recommended to be the preclinical species for further characterization prior to testing in humans. Finally, allometric scaling predicts human pharmacokinetic parameters would be acceptable for further development.

Introduction

Metabotropic glutamate receptors (mGluR) have received significant attention as therapeutic targets for the treatment of CNS disorders (Danysz, et al., 1995; Helton, et al., 1998; Cartmell, et al., 1999; Johnson et al., 2002, Takamori, et al., 2003). Unlike ionotropic glutamate receptors, which are ion channels, mGluRs are members of the G-protein coupled receptor superfamily and modulate synaptic transmission through second messenger systems that can both stimulate and inhibit neurons. The mGluR family of receptors is catalogued into 3 groups, consisting of 8 subtypes (Group I: mGluR1 and mGluR5, Group II: mGluR2 and mGluR3, and Group III: mGluR4, mGluR6, mGluR7, and mGluR8) (Nakanishi, 1992; Nakanishi and Masu, 1994; Pin and Duvoisin, 1995; Conn and Pin, 1997, Schoepp et al., 1999) and are located both pre- and post-synaptically.

Glutamate, the major excitatory amino acid in the CNS, binds mGluRs extracellularly thereby initiating intracellular cascade events. While Group I mGluRs are found primarily post-synaptically and ultimately increase neuronal excitability (Conn and Pin, 1997; Pin, et al., 1999, Milovanovic, et al., 2002), Group II and III mGluRs are primarily localized presynaptically and are coupled to the inhibitory G-proteins G_i and G_o , which reduce cellular levels of the second messenger c-AMP and inhibit glutamate release (Flor et al., 1995, Emile et al., 1996, Makoff et al., 1996, Conn and Pin, 1997; Pin et al., 1999, Kammermeier et al., 2003). Group II metabotropic glutamate receptors (mGluR2 and mGluR3), while not completely characterized, are thought to modulate neuronal excitability by regulating synaptic glutamate levels. Thus, agonists for these receptors are implicated in therapeutic indications including schizophrenia, anxiety, and addiction (Monn, et al., 1997; Helton et al., 1997; Helton et al., 1998; Moghaddam and Adams, 1998; Swanson and Schoepp, 2002) and have even advanced to the level of human clinical trials (Levine, et al., 2003).

MGS0028, the mGluR2/3 agonist, is a constrained glutamic acid analog (**Figure 1**) with *in vitro* potency at HmGluR2 and HmGluR3 of 0.57 and 2.07 nM, respectively (Nakazato, et al., 2000). *In vivo*, MGS0028 inhibits PCP induced head weaving behavior and hyperactivity in the rat at oral doses of 0.3 – 3 mg/kg (Nakazato, et al., 2000), and is active in the conditioned avoidance response model in rats over the same dose range (Takamori, et al., 2003). The desirable *in vitro* potency and *in vivo* efficacy profiles make this compound an attractive candidate for clinical development. Thus, to further characterize

DMD #4978

suitability and to select the appropriate preclinical species for future development, the metabolic and disposition profile in Sprague-Dawley rats, Beagle dogs, and Rhesus monkeys was characterized. Human pharmacokinetic (PK) parameters were predicted with allometric scaling methods. In addition, as brain penetration is required for an mGluR2/3 agonist to reach the intended target, analysis of brain penetration and brain levels over time in rats was carried out.

Methods

Materials. MGS0028 ((1R, 2S, 5S, 6S)-2-amino-6-fluoro-4-oxobicyclo[3.1.0]hexane-2,6-dicarboxylic acid monohydrate), MGS0034 ((1R, 2S, 4R, 5S, 6S)-2-amino-6-fluoro-4-hydroxybicyclo[3.1.0]hexane-2,6-dicarboxylic acid, the reductive metabolite of MGS0028) and MGS0025 (the 4S diastereomer of MGS0034) were synthesized at Taisho Pharmaceuticals Co. (Nakazato, A., et al., 2000). [¹⁴C]MGS0028 was synthesized by Amersham International (specific activity 9071.73 KBq/mg and radiochemical purity greater than 97% by TLC). The radioactive material was diluted with unlabeled compound synthesized by Taisho Pharmaceutical Co. when necessary. The chemical structures of the compounds and [¹⁴C]-labeled position on MGS0028 (indicated by an asterisk) are shown in **Figure 1**. Blank plasma was received from the following sources: rat plasma in EDTA, Pel Freeze Biologicals; dog plasma in EDTA, MRL-Rahway Beagle Facility; and Rhesus monkey plasma in EDTA, Biochem Pharmaceuticals. All solvents were purchased from Fisher in HPLC grade. The compounds are monohydrates and all data calculations were performed using the free-base molecular weight.

In vitro Metabolism. Rat and human liver microsomes were purchased from In Vitro Technologies (Baltimore, MD), and human liver microsomes were pooled from 10 individuals. Dog and rhesus monkey liver microsomes were obtained from MRL, Rahway and liver cytosol were obtained from MRL, West Point. Liver cytosol (1 mg/mL protein concentration) from rat, human, monkey and dog were incubated with 1 or 10 μM MGS0028 in the presence or absence of 1 mM NADPH (100 mM Tris buffer, pH 7.4). The reactions were terminated after 1 hr incubation at 37°C with the addition of two volumes of acetonitrile. Prior to LC-MS/MS analyses, the incubation samples were processed through solid phase extraction with Isolute SAX SPE columns (2 g/15 mL). MGS0028 and the metabolite MGS0034 were separated on a YMC ODS-4Q HPLC column (3 μm, 4.6x150 mm) with an isocratic mobile phase (95% water and 5% acetonitrile containing 0.1% acetic acid) at a flow rate of 0.5 mL/min. Tandem mass

DMD #4978

spectrometric (MS/MS) detection was carried out using electrospray (Micromass Quattro Ultima) in negative ion mode for the parent compound MGS0028 (m/z 216 \rightarrow 108), the metabolite MGS0034 (m/z 218 \rightarrow 154) and MGS0025, which is the 4S diastereomer of the metabolite.

Animal Experiments.

All animal experiments conducted at Merck Research Laboratories followed procedures set forth by the MRL Institutional Animal Care and Use Committee and all guidelines were in accordance with the NIH Guide for the Care and Use of Laboratory Animals. Experiments performed at Taisho Pharmaceutical Co. followed similar internal guidelines.

ADME Studies: Absorption, Tissue Distribution, Metabolism, and Excretion Using Radiolabel and Radioluminography in Rats.

Animals. Male Sprague-Dawley rats (8-9 weeks old) were obtained from Charles River, Japan. All animals were acclimated for at least one week prior to entering a study. The animals were provided with water and standard laboratory diet (MF, Oriental Yeast Co., Japan) *ad libitum* during acclimation, and were fasted overnight (about 18 hrs) before and 6 hr after dosing, except in the studies to examine the dietary effect and distribution of radioactivity after administration.

Dosing Solutions. [^{14}C]MGS0028 was dissolved in isotonic saline containing 0.3% Tween 80 for both intravenous (IV) and oral (PO) administration. The radiolabel doses and dosing volumes were 3.7 MBq/mL/kg for IV administration and 1.8-3.7 MBq/5mL/kg for PO administration. In the radioluminography studies, the radiolabel dosing volume was 7.4 MBq/5mL/kg.

Blood Concentrations of Radioactivity. Blood samples were taken from the tail vein at 2, 10 and 30 min, 1, 3, 6, 8 and 24 hr after IV administration of [^{14}C]MGS0028, and at 10, 20 and 30 min, 1, 2, 4, 6, 8 and 24 hr after PO administration. Each blood sample was solubilized with a mixture of 1 mL of Soluene-350 (Packard, USA) and 0.5 mL isopropanol, and decolorized by addition of 30 % H_2O_2 . Then 10 mL liquid scintillation cocktail (Hionic Fluor, Packard, USA) was added and the radioactivity was counted.

Radioluminography. After PO administration of [^{14}C]MGS0028, rats were sacrificed by ether anesthesia at 1, 4, 8 and 24 hr after dosing. The carcass was frozen in a dry ice-hexane mixture at approximately -80°C , embedded in 5% sodium carboxymethyl cellulose on microtome stage, and re-frozen. Forty micrometer thick sections were prepared by a Cryomacrocut (PMV450MP, LKB, Leica,

DMD #4978

Germany) and freeze-dried at -20°C. The sections were overturned in a protection membrane, placed in contact with an imaging plate (BAS-III, Fuji photo film, Japan), exposed under room temperature for 16 hr, and developed to prepare radioluminograms using a Bio-image analyzer (Model BAS2000, Fuji photo film, Japan). The section taken at 4 hr was also stained with hematoxylin-eosin.

Brain and CSF Concentrations of Radioactivity. After IV administration of [¹⁴C]MGS0028, rats were anesthetized with 125 mg/kg ketamine (Ketalar 50, Sankyo Co., Japan), and cerebro-spinal fluid (CSF) was collected from the cisterna magna at 1, 2, 4, and 6 hr; each aliquot was mixed with liquid scintillator and radioactivity counted. Blood was then collected from the abdominal aorta and the animals were decapitated immediately. Plasma was obtained by centrifugation of blood, then liquid scintillator was added and the radioactivity counted. Half of the cerebrum and cerebellum were excised and weighed. The Choroid plexus was removed from the other side of the cerebrum was put into scintillation counting vials for solubilization and the radioactivity counted. Brain tissues were homogenized in four volumes of saline and an aliquot of homogenate was weighed and solubilized with Soluene-350 and the radioactivity counted.

HPLC Analysis of Urinary Metabolite. Urine samples from rats receiving 1 mg/kg [¹⁴C]MGS0028 IV or PO were analyzed directly by radiometric HPLC after filtration. The filtrate was introduced onto a cation exchange column (Hypersil Duet Cation 5µm, 150 x 4.6 mm) and eluted with acetonitrile:water (ratio 2:98 containing 5% TFA) at a flow rate of 0.8 mL/min. Radioactivity was detected by a radioactive monitor (Ramona93, Raytest, Germany).

LC/MS Analysis of Urinary Metabolite. Rat urine (0.1 mL, 0-8 hr post 1 mg/kg PO dose) was mixed with 1 mL of methanol containing 1% trichloroacetic acid and centrifuged at 11,000 g for 10 min. The supernatant was dried under a gentle stream of nitrogen and the residue dissolved in 0.1 mL of acetonitrile and subjected to derivatization. The PFB derivatives of MGS0028 and its metabolite(s) were prepared by addition of pentafluorobenzyl bromide (0.1 mL) and diisopropylethylamine (0.1 mL) followed by vigorous mixing and heating at 70°C for 2 hr. The derivatization was terminated by evaporation of reagents under a gentle stream of nitrogen. The residue was dissolved in 0.2 mL acetonitrile and an aliquot (30 µL) was injected onto a HPLC system (LC10A, Shimadzu) with a reverse-phase column (Capcel-pak ODS, 5 µm, 4.6 x 150 mm, Shiseido). The analyte was eluted with a linear gradient (38% to

DMD #4978

90% ACN over 30 min) at a flow rate of 1.0 mL/min; the eluent was collected in 1.0 mL fractions and each fraction was measured for radioactivity. The fraction corresponding to the peaks of PFB derivatives of [¹⁴C]MGS0028 and the metabolite were analyzed by a LC/MS/MS system (API3000 mass spectrometer; Perkin Elmer Sciex, Ontario, Canada).

Urinary and Fecal Excretion of Radioactivity. Fasted rats were individually housed in glass metabolic cages after IV or PO administration of [¹⁴C]MGS0028. Urine was collected separately over the periods of 0-8, 8-24, 24-48, 48-72 hr and feces were collected in 24 hr intervals until 72 hr. After collection, each fraction was weighed. An aliquot of each urine sample was mixed with liquid scintillator and the radioactivity counted. The feces were homogenized and solubilized with Soluene-350 and the radioactivity counted.

Measurement of Radioactivity. Radioactivity in each test sample was measured by a liquid scintillation counter (LS6000TA, Beckman, USA). Quenching was corrected by means of the external standard method. Concentrations of radioactivity were expressed as concentration equivalents based on the specific activity in the dosing solution.

Pharmacokinetic Studies in Rats, Dogs, and Monkeys.

Animals. Male Sprague-Dawley rats (Harlan, San Diego) were habituated to the vivarium for at least three days before entering a study. Jugular vein cannulae were implanted for serial bleeding and the animals were allowed to recover for an additional two days. MGS0028 was administered IV at 3 and 10 mg/kg (0.3% Tween 80 in saline, 0.5 mL/kg, n=3) and PO at doses of 1, 3 and 10 mg/kg (0.3% Tween 80 in water, 2 mL/kg, n=3). Blood samples were collected at 5 (IV only), 15 and 30 min, 1, 2, 4, 6, 8 and 24 hr post-dose.

Male Rhesus monkeys, weighing 8-10 kg were fasted for 18 hr prior to dosing and 8 hr thereafter. The animals received an IV dose of MGS0028 at 1 mg/kg (saline, 0.1 mL/kg, n=3) and a PO dose at 5 mg/kg (water, 5 mL/kg, n=3). Blood samples were collected at 0, 5 (IV only), 15 and 30 min, 1, 2, 4, 6, 8 and 24 hr post-dose. Male Beagle dogs weighing 10-12 kg were fasted for 18 hr prior to dosing and 4 hr thereafter. The animals received an IV dose of MGS0028 at 0.3 mg/kg (saline, 0.1 mL/kg, n=3). Prior to the oral study, the dogs were pre-treated with MGS0028 at 0.1 mg/kg/day PO for three days to allow the animals to develop tolerance to the potential emetic effect of MGS0028. Before the study day, the

DMD #4978

animals were fasted over night and received a dose of MGS0028 at 0.1 or 0.3 mg/kg PO (water, 5 mL/kg, n=3). Blood samples were collected at 0, 5 (IV only), 15 and 30 min, 1, 2, 4, 6, 8 and 24 hr post-dose. In all cases, the plasma samples were obtained upon centrifugation of blood samples and stored at -20°C until analyzed.

LC-MS/MS Assay. A LC-MS/MS method was developed for the simultaneous analysis of non-derivatized MGS0028 and the reductive metabolite MGS0034. Plasma samples (50 μ L), calibration and QC standards underwent a protein precipitation procedure on a Tomtec robotic system in 96-well plate format. Calibration curves for both MGS0028 and MGS0034 were prepared in species matched blank plasma with a typical dynamic range of 2-2000 ng/mL (higher if required). In cases where the metabolite standard was unavailable, the stereo isomer, MGS 0025, was used as a surrogate. LY 379268 was used as the analytical internal standard, which was spiked in the precipitation solvent. After removal of the protein pellets, the samples were processed in one of two ways: 1) the samples were diluted with two volumes of 0.05% formic acid and 100 μ L of the final mixture injected onto the LC-MS/MS system or 2) the samples were further purified by solid phase extraction using strong-anion exchange (SAX) cartridges (96-well plate format, 25 mg capacity Isolute SAX cartridges, obtained from Jones Chromatography). Washing steps included methanol, water, acetonitrile/water (9:1) at 400 μ L each, followed by elution with 400 μ L of acetonitrile/water (9:1) containing 1% TFA. The final eluent was either injected directly or after drying and reconstitution in 100 μ L of 0.05% formic acid (5 μ L).

Samples prepared by method 1 were analyzed by liquid chromatography with mass detection on a 50 x 4.6 mm Phenomenex AQUA column (polar end-capped C18) using isocratic elution at 95% water containing 0.05% formic acid and 5% acetonitrile at 0.8 mL/min. The eluent was split 4:1 such that <0.2 mL/min was flowing into the mass spectrometer. For samples prepared using SAX after protein precipitation (method 2), chromatographic separation was achieved on a 150 x 2 mm YMC Hydrosphere column (polar end-capped C18) with the same isocratic mobile phase elution at a flow rate of 0.2 mL/min. Tandem mass spectrometric (MS/MS) detection was carried out using electrospray (Micromass Quattro Ultima) in negative ion mode for the parent compound MGS0028 (m/z 216 \rightarrow 108), the metabolite MGS0034 (m/z 218 \rightarrow 154) and I.S. (m/z 186 \rightarrow 98.5). The lower limit of quantitation (LOQ) ranged from 4 to 32 ng/mL (0.02 – 0.15 μ M), and was assay dependent.

DMD #4978

Calculation of Pharmacokinetic Parameters. Pharmacokinetic parameters were calculated using a template developed in-house. Calculations are based on the non-compartmental model using the linear trapezoidal estimation method.

The dose normalized AUC ($\mu\text{M}\cdot\text{hr}$) is defined as $\text{AUCN} = \text{AUC}/\text{Dose}$ and the area under the moment curve ($\mu\text{M}\cdot\text{hr}$) for I.V. experiments is calculated as,
$$\text{AUMC} = T(1)^2 \cdot C(1)/2 + \sum_2^N (T(n) - T(n-1)) \cdot (T(n) \cdot C(n) + T(n-1) \cdot C(n-1))/2 - C(N) \cdot T(N)/S + C(N)/S^2$$

where the last two terms are omitted when the extrapolation terms in AUC are omitted. The concentration at time zero, C_0 (μM), will be 0 after a compound is dosed orally or by infusion.

Plasma Protein Binding and Blood/Plasma Partition.

Rat, dog, monkey and human plasma were spiked with [^{14}C]MGS0028 at concentrations of 1 and 10 μM . Aliquots (200 μL , $n = 3$ per concentration) were transferred to ultracentrifuge tubes and centrifuged for 60 minutes at 1,800 g at 37°C. An aliquot of the supernatant (50 μL) from each tube was mixed with 10 mL Pico-Fluor 40 and counted with a liquid scintillation counter.

Fresh blood from male Sprague-Dawley rats and humans was spiked with [^{14}C]MGS0028 at a concentration of 1 μM . These samples were incubated at 37°C. A preliminary study established that 5 min was sufficient to reach equilibrium. Aliquots were taken and centrifuged to separate the plasma from red blood cells. Plasma (100 μL) was dissolved in scintillant and counted with a Beckman Scintillation Counter LS6500.

Allometric Scaling of Pharmacokinetics Parameters. The effective human half-life ($T_{1/2}$) was assumed to be 1 hr, as this value was consistent for all preclinical species tested. The human PK parameters for plasma clearance (Cl_p) and volume of distribution (V_d) were calculated using protocols described by Obach, et al. (Obach, et al., 1997). Methods used for V_d included V2, V3a, and V3b. For Cl_p , methods C3b, C3c, and C3d were used, as well as the average predicted human V_d (0.09 L/kg) using the formula $\text{Cl}_p = (0.693 \cdot V_d)/T_{1/2}$.

Results

Absorption. MGS0028 was found to be well absorbed in rats following oral (PO) dosing of [^{14}C]MGS0028. Pharmacokinetic parameters derived from the total radioactivity are summarized in **Table**

DMD #4978

1. Upon an intravenous (IV) dose of 1 mg/kg [^{14}C]MGS0028, total radioactivity reached 5.91 μM equivalents at the first sampling point of 2 minutes and declined bi-exponentially thereafter with a half-life ($T_{1/2}$) of 2.4 hrs. To assess the impact of food, [^{14}C]MGS0028 was administered orally to both fasted and fed rats. Following a PO dose of 1 mg/kg [^{14}C]MGS0028 to fasted rats, total radioactivity peaked at 1.15 μM equivalents at 0.8 hr post-dose. In fed animals, the absorption process was noticeably slower peaking at a lower level and at a later time (0.49 μM equivalents at 1.7 hr). Nonetheless, the $\text{AUC}_{0-24\text{hr}}$ values were similar in fasted and fed animals (3.40 and 3.63 $\mu\text{M}\cdot\text{hr}$) and absorption was good with about 60% bioavailability.

Tissue distribution. Distribution of radioactivity to tissues following a dose of 1 mg/kg PO [^{14}C]MGS0028 was examined by radioluminography. At 1 hr post-dose, relative levels of radioactivity were ranked in four groups: kidney, bladder urine, intestinal contents, thymus, liver and Harderian gland > blood, lung, and skin > heart, testis, epididymis, pancreas, submandibular gland, adrenal gland, spleen, and small intestine >> cerebrum and cerebellum (undetectable). Although most parts of the brain contained an undetectable level of radioactivity, the area postrema showed a relatively high level of radioactivity (**Figure 2**). The localization of radioactivity was confirmed with hematoxylin-eosin staining of the slice. At 4 hr post-dose, radioactivity was detected in kidney, bladder urine, intestinal contents, thymus, liver, pancreas, and Harderian gland, which all appeared to be higher than that in the blood. At 8 hr post-dose, radioactivity was detected in all the listed tissues with the exception of the pancreas. At 24 hr post-dose, radioactivity could still be detected in the kidney, intestinal contents, thymus, liver, and the Harderian gland.

To further characterize CNS penetration, the distribution of radioactivity in the brain, choroid plexus, and cerebro-spinal fluid (CSF), relative to blood and plasma was studied in rats following a dose at 1 mg/kg IV [^{14}C]MGS0028. As shown in **Figure 3**, levels of radioactivity in the plasma, cerebrum and CSF reached 0.87, 0.06, and 0.02 μM equivalents at 1 hr post-dose, respectively. The brain to plasma ratio of radioactivity was 0.07 at 1 hr, corresponding to the maximum plasma concentration (C_{max}), and 0.39 at 6 hr. The elimination of the radioactivity in the brain was slower than in the plasma and CSF. No radioactivity was detected in the choroid plexus.

DMD #4978

Metabolism. *In vivo* metabolism of [¹⁴C]MGS0028 was studied in rats following a dose at 1 mg/kg PO in fasted rats. **Figure 4** shows the radio-chromatograms of rat urine samples, which demonstrated the presence of a single major metabolite. The metabolite consisted of 90% of the total radioactivity in 0-8 hr urine samples, and was the only peak detected in 8-24 hr urine samples. Identification of the metabolite was carried out by derivatization with pentafluorobenzoylbromide (PFB), followed by LC-MS with APCI detection. The [MH]⁺ of the derivatized metabolite (M1-3PFB) was at m/z 760, which was 2 amu higher than the parent drug (MGS0028-3PFB) at m/z 758, indicating the metabolite contained an alcohol group as a result of metabolic reduction of the ketone. Subsequently, two diastereoisomers of the alcohol were synthesized: MGS0025 (4S-isomer) and MGS0034 (4R-isomer) (Nakazato et al., 2000). After derivatization with PFB and HPLC separation, retention time comparison to authentic standard demonstrated MGS0028 was stereospecifically metabolized in rats to from the 4R isomer (MGS0034). MGS0034 was also identified in monkey plasma, whereas it was not detected in dog plasma or urine.

For species comparison, the *in vitro* metabolism of MGS0028 was investigated with rat, monkey (Rhesus), dog and human liver sub-cellular fractions (microsomes and cytosol). MGS0028 was stable in hepatic microsomal incubations across the four species and the reductive metabolite MGS0034 was not detected in liver microsomal incubations (data not shown). However, the metabolite was stereospecifically formed in rat, monkey, and human liver cytosols, which suggested the reductive metabolism of MGS0028 was mediated by cytosolic carbonyl reductase. Interestingly, the metabolite was not formed in dog cytosol. The rate of the formation was quantitatively assessed at a pharmacologically relevant concentration (1 μM) (**Figure 5**). The rate of MGS0034 formation was the most rapid in monkey cytosol at 82.6 pmol/mg/hr, whereas the formation rate in rat and human cytosol was approximately 18 times slower. This rank order is consistent with the extent of *in vivo* formation of MGS0034 measured in PK studies. In all three species, only one stereoisomer was found and the retention time was consistent with the synthetic standard MGS0034 (**Figure 6**). This finding suggests the formation of MGS0034 is highly stereoselective and is consistent across these species.

Excretion. Following an IV dose of [¹⁴C]MGS0028 at 1 mg/kg in rats, the majority (90.8%) of the radioactivity was excreted in urine with only 4.7% eliminated in feces. A similar excretion pattern was

DMD #4978

observed after PO dosing, i.e., 93% in urine and 3.9% in feces (**Table 2**). Comparable urinary excretion after IV and PO administration suggests total radioactivity was primarily eliminated through renal clearance.

Pharmacokinetics in rats, monkeys, and dogs. For all species, plasma levels were quantitatively measured for both MGS0028 and the reductive metabolite MGS0034. The PK parameters in rats, as well as dogs and monkeys, are provided in **Table 3**, and the rat plasma concentration-time curves at 3 mg/kg are shown in **Figure 7**. In rats, following administration of MGS0028 at 3 mg/kg IV, mean plasma clearance (Cl_p) is moderate at 16.2 mL/min/kg and the corresponding volume of distribution (V_d) value is 0.5 L/kg, which is nearly on the order of total body water. Oral bioavailability and dose proportionality studies in rats were conducted at 1, 3 and 10 mg/kg. The corresponding mean C_{max} values were 1.0, 2.7, and 6.0 μ M and exposure, as measured by $AUC_{0-24\text{ hr}}$, increased proportionally with the increase in dose. At all doses, oral bioavailability was greater than 60%. In both IV and PO dose studies, the reductive metabolite MGS0034 was detected, and the metabolite to parent drug AUC ratio was variable, ranging from 0.3 to 0.8.

The PK parameters measured in Rhesus monkeys are provided in **Table 3**, and the plasma concentration-time curves are shown in **Figure 8**. Following administration of 1 mg/kg IV MGS0028, the Cl_p was modest at 8.0 mL/min/kg and the mean V_d was at 0.6 L/kg (nearly the volume of total body water). Again, an effective $T_{1/2}$ of 1 hr was observed. A study was conducted at 5 mg/kg PO in solution (water), resulting in a mean C_{max} of 1.0 μ M. Following PO dosing, plasma levels of MGS0028 are sustained for at least 8 hr, presumably due to slow absorption, yet bioavailability was relatively modest at only about 20%. The reductive metabolite MGS0034 was found in relatively high abundance in plasma, reaching levels comparable to or exceeding the parent drug beyond 4 hrs post-dose. The AUC ratio between the metabolite and the parent drug was 0.3 and 0.9 following IV and PO administration, respectively.

The dog PK parameters and plasma concentration-time curves are shown in **Table 3** and **Figure 9**. Following administration of MGS0028 at 0.3 mg/kg IV, Cl_p and V_d were low at 2.8 mL/min/kg and 0.1 L/kg, respectively, and the effective $T_{1/2}$ was consistently short at 1 hr. Oral studies were conducted at two doses, 0.1 and 0.3 mg/kg, both given in solution using 0.3% Tween 80 in water, following three days

DMD #4978

of administration at 0.1 mg/kg PO to minimize compound induced emesis. Plasma taken prior to compound administration on the study day concluded there was no measurable compound present from pre-dosing. Mean C_{max} values increased nearly proportionally from 0.1 mg/kg to 0.3 mg/kg, at 1.5 μ M and 4.0 μ M. Oral bioavailability was about 60% to 70%. In dogs, the reductive metabolite MGS0034 was not detected in plasma following either IV or PO administration. Furthermore, urine samples collected after IV administration also lacked the metabolite.

Plasma Protein Binding and Blood/Plasma Partition. The mean plasma protein binding values in three animal species and humans are provided in **Table 4**. At a pharmacologically relevant concentration (1 μ M), the mean unbound fraction in rat, dog, monkey (Rhesus) and human plasma was near 70% (similar values were obtained at 10 μ M). Thus, the plasma protein binding of MGS0028 is very low in all four species. The blood to plasma partition of MGS0028 was 0.76 ± 0.02 and 0.64 ± 0.02 in rats and humans, respectively. A time course study indicated the equilibrium between plasma and red blood cells was reached by 5 minutes at 37°C. The blood to plasma ratio (slightly above 0.5) suggests MGS0028 is primarily partitioned into plasma rather than red blood cells.

Allometric Scaling of Pharmacokinetic Parameters. The human PK parameters for Cl_p and V_d were predicted using allometric scaling of the PK data from the preclinical species examined. The measurable effective $T_{1/2}$ in all three preclinical species was about 1 hr, thus $T_{1/2}$ in human was assumed to be the same for the purpose of scaling. The other PK parameters were fitted using a number of methods to predict ranges (Obach, et al., 1997). All methods resulted in fairly narrow ranges which are presented in **Table 5**. Human Cl_p is predicted to be modest, at between 1 - 4 mL/min/kg (**Figure 10**). Volume of distribution is also predicted to be low, at 0.08 - 0.11 L/kg, indicating a preference for the blood compartment.

Discussion

MGS0028 is a group II metabotropic glutamate receptor agonist with improved potency (EC_{50} at HmGluR2 and HmGluR3 is 0.57 nM and 2.07 nM, respectively) over current compounds in its class, including the leading clinical candidate, LY354740 (EC_{50} 18.3 nM and 62.8 nM in the same assay) (Nakazato, A., et al., 2000, Johnson, et al., 2002). LY354740 established proof of concept for anxiety in humans for mGluR2/3 agonists, showing efficacy in the CO₂ induced anxiety model and fear potentiated

DMD #4978

startle response in humans (Levine et al., 2003, Grillon et al., 2003). At present, MGS0028 has demonstrated efficacy in animal models of schizophrenia and anxiety, including the PCP induced hyperactivity and fear avoidance models in rats (Nakazato, A., et al., 2000, Takamori, et al., 2003). Having established desirable *in vitro* potency and *in vivo* efficacy, further analysis of the metabolism and disposition of MGS0028 was done to determine if MGS0028 would be an attractive candidate for clinical development. Thus, rat ADME and preclinical multi-species PK was examined and scaled using allometric methods to predict key human PK parameters.

Since mGluR2/3 receptors are located in the brain, special emphasis was given to brain penetration and localization when analyzing of total body distribution. Rat ADME and multi-species PK analysis of MGS0028 indicate this compound is well absorbed in all preclinical species and is widely distributed. However, for a CNS drug, MGS0028 is poorly brain penetrant. This is probably due to the polarity of MGS0028, as it was found to not be a Pgp substrate and suffers from poor permeability (data not shown). MGS0028 is highly water soluble and distribution studies in rat show it is distributed throughout various tissues, urine, and intestinal contents by 1 hr (1 mg/kg PO [¹⁴C]MGS0028, as measured by radioactivity). However, in the brain, rat whole body radioluminography only detected radioactivity in the area postrema. Subsequent studies utilizing LC with radioactive detection measured brain (cerebrum and cerebellum), CFS, choroid plexus, blood, and plasma levels over time after administration at 1 mg/kg IV [¹⁴C]MGS0028. Radioactivity was detectable in all tissues except the choroid plexus, suggesting that the blood cerebrospinal fluid barrier is not a major route for MGS0028 entry into the brain. Additionally, brain levels only reach approximately 50 nM by 1 hr in rat yielding a brain-to-plasma ratio of < 0.4 at all time points tested (1-6 hr). Even so, brain levels were well above the IC₅₀ for both mGluR2 and mGluR3. This result is not too surprising, as most small, polar compounds are poorly brain permeable. However, transporters in the blood-brain barrier regulate entry of amino acids and peptides providing a means of entry into the brain maintaining homeostasis (Gottlieb, et al., 2003; Zlokovic, et al., 1992; Oldendorf and Szabo, 1976). Being a glutamate analog, MGS0028 may be actively transported into the brain by an amino acid transporter, specifically the glutamate transporter. Endogenous glutamate levels in brain persist at about a 50-fold lower concentration than in plasma (1-10 μM in brain and 40-60 μM in plasma) and brain levels are maintained by both active influx and efflux

DMD #4978

transporters (Gottlieb, et al., 2003; Oldendorf and Szabo, 1976). Interestingly, MGS0028 enters the brain rapidly, when plasma levels are highest (0.1 μM in brain and 1 μM in plasma), suggesting at high plasma concentrations there is enough compound present to compete with glutamate at these transporters.

Another important finding was elimination from the brain is slower than from plasma. Thus, even though total brain exposure to MGS0028-derived compounds is very low at efficacious doses (\sim 0.3-3 mg/kg) (Nakazato, et al., 2000, Takamori, et al., 2003) and penetration is low when compared to plasma C_{max} (< 0.1), slow brain elimination might prolong the duration of action. Whilst this effect may be a benefit, it also has the unfortunate effect of undermining the ability to track pharmacodynamic readouts with plasma levels, an important consideration for future development. The slower elimination of MGS0028 from the brain than from plasma would suggest MGS0028 either is not a substrate for glutamate efflux transporters, or that competition with endogenous glutamate results in slow efflux transport kinetics. If MGS0028 is not a substrate for efflux transporters, then its poor membrane permeability would prevent easy passage back into the blood stream, resulting in prolonged elimination from the brain.

In vivo studies revealed that MGS0028 metabolism was species dependent. In rats and monkeys, MGS0028 is stereospecifically metabolized to a single reductive metabolite, MGS0034, which has been characterized as the 4R-isomer (Figures 1 and 3) by comparison to authentic synthetic standards of both the 4R and 4S derivatives. While in dogs, MGS0028 metabolism is not detected. To assist in the selection of preclinical safety species, *in vitro* metabolic studies were done using liver sub-cellular fractions from four species (rat, dog, monkey, and human) to correlate with the *in vivo* analysis. *In vitro* studies revealed the reductive metabolism occurred in cytosol, but not in microsomes, thus MGS0028 is most likely reduced to MGS0034 by a carbonyl reductase, a NADPH dependent cytosolic enzyme (Oppermann and Maser, 2000; Forrest and Gonzalez, 2000). Carbonyl reductase is known to stereospecifically reduce xenobiotic aliphatic ketones, such as warfarin, via an acid-base mechanism (Oppermann and Maser, 2000; Hermans J. J. and Thijssen H. H., 1992). However, further studies are required to understand the reason why MGS0028 is not metabolized in dogs (Forrest and Gonzalez, 2000).

DMD #4978

In vivo and *in vitro* metabolism correlated for all three preclinical species, including the relative abundance of metabolite formed. The *in vitro* rank order of metabolism was found to be monkey >> rat ~ human >> dog, whereas the *in vivo* rank order was monkey >> rat >> dog. Thus, it is predicted the reductive metabolite will be present in humans, since the metabolite was formed in human liver cytosol incubations. Additionally, excretion studies in rat showed the majority of radioactivity was excreted in urine as the metabolite (90% in 0-8 hr urine post 1 mg/kg PO [¹⁴C]MGS0028), indicating the primary route of elimination in rats was reductive metabolism.

As with metabolism, there were significant differences in the PK response across the three species tested. In rats and monkeys, Cl_p is moderate (rat: 16.6 mL/min/kg at 3 mg/kg, monkey: 8.0 mL/min/kg at 1 mg/kg) and the V_d is on the order of total body water, correlating to wide distribution (0.5 L/kg and 0.6 L/kg, respectively). However, in dogs both Cl_p and V_d are low (2.8 mL/min/kg and 0.1 L/kg at 0.3 mg/kg). Oral bioavailability is good in rats and dogs (>60% in both species), but lower in Rhesus monkeys (20%). Based on quantitative results, the effective $T_{1/2}$ was determined to be about 1 hr in all species examined, however qualitative data indicates a longer terminal phase, representing a minor portion of the total AUC (< 1%, data not shown). MGS0028 is primarily partitioned into plasma (blood to plasma ratio 0.74 and 0.64, in rat and human, respectively), and is not highly bound to plasma proteins (approximately 70% unbound in rat, dog, Rhesus, and human). Thus, protein binding should not affect the pharmacological activity or highly impact prediction of human PK. Assuming $T_{1/2} = 1$ hr in human, allometric scaling to human PK parameters predicts that MGS0028 will have a low V_d (~0.1 L/kg), and low Cl_p (~1-4 mL/min/kg). It is difficult to interpret the impact of the short effective $T_{1/2}$ on the pharmacologic action of MGS0028, due to the extended $T_{1/2}$ expected in brain. Further studies are needed to understand brain elimination, including taking data at later time-points (> 6 hr) and after chronic dosing.

In summary, the reductive metabolism of MGS0028 was found to be species dependent. A single major reductive metabolite (MGS0034) was observed in rats and monkeys, while no metabolite was detected in dogs. *In vitro* metabolic studies in rat, dog, monkey, and human liver cytosols were consistent with *in vivo* results and indicate reductive metabolism may occur in humans. Thus, it is recommended that further preclinical development of MGS0028 be done in rats and monkeys. Based on the PK

DMD #4978

parameters of MGS0028 in the three preclinical species studied (rats, dogs, and monkeys), it was predicted with allometric scaling methods that MGS0028 would have acceptable human Cl_p and overall PK parameters.

Acknowledgments

We thank Kazunari Sakagami (TPC) for helpful synthesis, and Manabu Itho (TPC) for support analysis, Masayo Yamazaki (MRLWP) for helpful discussions, and John Hutchinson (MRLSD) for advice and review.

DMD #4978

References

- Cartmell, J., Monn, J. A., and Schoepp, D. D. (1999) The metabotropic glutamate 2/3 receptor agonists LY354740 and LY379268 selectively attenuate phencyclidine versus D-amphetamine motor behaviors in rats. *J. Pharmacol. Exp. Ther.* **291**:161-170.
- Conn, J.-P. and Pin, P.J. (1997) Pharmacology and functions of metabotropic glutamate receptors. *Ann. Rev. Pharmacol. Toxicol.* **37**:205-237.
- Danysz W., Parson, C. G., Bresink, I., and Quack, G. (1995) Glutamate in CNS disorders. *Drug News Perspect.* **8**:261-277.
- Emile, L., Mercken, L., Apioe, F., Pradier, L., Bock, M.-D., Menager, J., Clot, J., Doble, A., Blanchard, J.-C. (1996) Molecular cloning, functional expression, pharmacological characterization, and chromosomal localization of the human metabotropic glutamate receptor type 3. *Neuropharmacology* **35**:523-530.
- Flor, P.J., Lindauer, K., Puttner, I., Ruegg, D., Lukic, S., Knopfel, T., Kuhn, R. (1995) Molecular cloning, functional expression and pharmacological characterization of human metabotropic glutamate receptor type 2. *European Journal of Neuroscience* **7**:622-629.
- Forrest, G. L. and Gonzalez, B. (2000) Carbonyl reductase. *Chem-Biol. Interactions* **129**:21-40.
- Gottlieb, M., Wang, Y., and Teichberg, V.I. (2003) Blood-mediated scavenging of cerebrospinal fluid glutamate. *J. Neurochem.* **87**:119-126.
- Grillon, C., Cordova, J., Levine, L.R., and Morgan, C.A. 3rd. (2003) Anxiolytic effects of a novel group II metabotropic glutamate receptor agonist (LY354740) in the fear potentiated startle paradigm in humans. *Psychopharmacology* **168**:446-454.
- Helton, D.R., Taizzano, J.P., Monn, J.A., Schoepp, D.D., Kallman, M.J. (1997) LY354740: a metabotropic glutamate receptor agonist which ameliorates systems of nicotine withdrawal in rats. *Neuropharmacology* **36**:1511-1516.
- Helton, D.R., Taizzano, J.P., Monn, J.A., Schoepp, D.D., Kallman, M.J. (1998) Anxiolytic and side-effect profile of LY354740: a potent, highly selective, orally active agonist for group II metabotropic glutamate receptors. *J. Pharmacol. Exp. Ther.* **284**:651-660.
- Hermans J.J. and Thijssen H.H. (1992) Stereoselective acetyl side chain reduction of warfarin and analogs. Partial characterization of two cytosolic carbonyl reductases. *Drug Metab. Dispos.* **20**(2):268-274.
- Johnson, J.T., Mattiuz, E.L., Chay, S.H., Herman, J.L., Wheeler, W.J., Kassahun, K., Swanson, S.P., Phillips, D.L. (2002) The disposition, metabolism, and pharmacokinetics of a selective metabotropic glutamate receptor agonist in rats and dogs. *Drug Metab. Dispos.* **30**:27-33.
- Kammermeier, P.J., Davis, M.I., and Ikeda, S.R. (2003) Specificity of metabotropic glutamate receptor 2 coupling to G proteins. *Mol. Pharmacol.* **63**:183-191.
- Levine, L. (2003) The mGlu2/3 Receptor Agonist, LY354740, Reduces Panic Anxiety Induced by A CO2 Challenge in Patients Diagnosed with Panic Disorder. Poster Anxiety Disorders Association of America.
- Levine, L.R., Gaydos, B., Sheehan, D.V., Goddard, A., Feighner, J., Potter, W.Z., and Schoepp, D.D. (2003) LY354740, an MGLU2/3 Receptor Agonist, Reduces CO2-Induced Panic Anxiety in Patients Diagnosed with DSM-IV Panic Disorder. Poster NCDEU.

DMD #4978

Makoff, A., Volpe, F., Lechuk, R., Harrington, K., Emson, P. (1996) Molecular characterization and localization of human metabotropic glutamate receptor type 3. *Molecular Brain Research* **40**:165-170.

Milovanovic, D. R., Dejanovic, S. D., Mihajlovic, G., and Jankovic, S. M. (2002) A Concise Review of Glutamatergic Neurotransmission. *Epitheorese Klinikes Farmakologias Kai Farmakokinetikes, International Edition* **15**:125-136.

Moghaddam, B. and Adams, B.W. (1998) Reversal of phencyclidine effects by a group II metabotropic glutamate receptor agonist in rats. *Science* **28**:1349-1352.

Monn, J.A., Valli, M.J., Massey, S.M., Wright, R.A., Salhoff, C.R., Johnson, B.G., Howe, T., Alt, C.A., Rhodes, G.A., Robey, R.L., et al. (1997) Design, synthesis, and pharmacological characterization of (+)-2-aminobicyclo[3.1.0]hexane-2,6-dicarboxylic acid (LY354740): a potent, selective, and orally active group 2 metabotropic glutamate receptor agonist possessing anticonvulsant and anxiolytic properties. *J. Med. Chem.* **40**:528-537.

Nakanishi, S. (1992) Molecular diversity of glutamate receptors and implications for brain function. *Science (Wash. DC)* **258**:597-603.

Nakanishi, S. and Masu, M. (1994) Molecular diversity and functions of glutamate receptors. *Annu. Rev. Biophys. Biomol. Struct.* **23**:319-348.

Nakazato, A., Kumagai, T., Sakagami, K., Yoshikawa, R., Suzuki, Y., Chaki, S., Ito, H., Taguchi, T., Nakanishi, S., and Okuyama, S. (2000) Synthesis, SARs, and Pharmacological Characterization of 2-Animo-3 or 6-fluorobicyclo[3.1.0]hexane-2,6-dicarboxylic Acid Derivatives as Potent, Selective, and Orally Active Group II Metabotropic Glutamate Receptor Agonists. *J. Med. Chem.* **43**:4893-4909.

Obach, R. S., Baxter, J. G., Liston, T. E., Silber, M., Jones, B. C., MacIntyre, F., Rance, D. J., and Wastall, P. (1997) The Prediction of Human Pharmacokinetic Parameters from Preclinical and *In vitro* Metabolism Data. *JPET* **283**:46-58.

Oldendorf, W.H. and Szabo, J. (1976) Amino acid assignment to one of three blood-brain barrier amino acid carriers. *Am. J. Phys.* **230**(1):94-98.

Oppermann, U. C. T. and Maser, E. (2000) Molecular and structural aspects of xenobiotic carbonyl metabolizing enzymes. Role of reductases and dehydrogenases in xenobiotic phase I reactions. *Toxicology* **144**:71-81.

Pin, J.-P. and Duvoisin, R. (1995) The metabotropic glutamate receptors: structure and function. *Neuropharmacology* **34**:1-26.

Pin, J.-P., De Colle, C., Bessis, A.-S., and Acher, F. (1999) New Perspectives for the development of selective metabotropic glutamate receptor ligands. *Eur. J. Phar.* **375**:277-294.

Schoepp, D.D., Jane, D.E., and Monn, J.A. (1999) Pharmacological agents acting at subtypes of metabotropic glutamate receptors. *Neuropharmacology* **38**:1431-1476.

Schoepp, D.D., Wright, R.A., Levine, L.R., Gaydos, B., and Potter, W.Z. (2003) LY354740, an mGlu2/3 Receptor Agonist as a Novel Approach to Treat Anxiety/Stress. *Stress* **6**(3):189-197.

Swanson, C.J. and Schoepp, D.D. (2002) The group II metabotropic glutamate receptor agonist (-)-2-Oxa-4-aminobicyclo[3.1.0]hexane-4,6-dicarboxylate (LY379268) and clozapine reverse phencyclidine-induced behaviors in monoamine-depleted rats. *JPET* **303**:919-927.

DMD #4978

Takamori, K., Shiho, S., Chaki, S., and Tanaka, M. (2003) Antipsychotic action of selective group II metabotropic glutamate receptor agonist MGS0008 and MGS0028 on conditioned avoidance responses in the rat. *Life Sciences* **23**:1721-1728.

Zlokovic, B.V., McComb, J.G., Perlmutter, L., Welss, M.H., and Davson, H. (1992) Neuroactive peptides and amino acids at the blood-brain barrier: Possible implications for drug abuse. In: Frankenheim, J. and Brown, R.M., eds. *Bioavailability of drug to the brain and the blood-brain barrier. Research monograph 120*. National Institute on Drug Abuse, pp. 26-42.

DMD #4978

Figure 1. Chemical structures of MGS0028, the metabolite MGS0034, and the stereoisomer of the metabolite, MGS0025. The asterisk (*) indicates the position of the radio-label.

Figure 2. Radioluminogram of a rat brain 4 hr after oral administration of [¹⁴C]MGS0028 at 1 mg/kg. The radiolabel dosing volume was 7.4 MBq/5mL/kg. Radioactivity was only detected in the area postrema. The localization of radioactivity was confirmed with hematoxylin-eosin staining of the slice.

Figure 3. Radioactivity in rat blood, plasma, brain, and CSF following IV administration of [¹⁴C]MGS0028 (3.7 MBq/mL/kg). Each point represents the mean ± SD of three animals.

Figure 4. Representative radio-HPLC chromatograms of urine collected during 0-8 and 8-24 hr after an oral dose of [¹⁴C]MGS0028 to rats at 1 mg/kg. [¹⁴C]MGS0028 was dissolved in isotonic saline containing 0.3% Tween 80 (1.8-3.7 MBq/5mL/kg).

Figure 5. *In vitro* formation rates of MGS0034 from MGS0028 in hepatic cytosols. 1 uM MGS0028 was incubated at 37 °C for 1 hr. Protein concentration was 1 mg/mL.

Figure 6. Confirmation of stereoselective formation of MGS0034 from MGS0028. The LC-MS/MS chromatograms for the parent → daughter transition of MGS0028 and the parent + 2 amu → daughter transition of the metabolite. The top trace is from *in vitro* metabolism in monkey cytosol, while the bottom trace is a mixture of authentic standards for MGS0028, MGS0034, and the stereoisomer, MGS0025.

Figure 7. MGS0028 and metabolite (MGS0034) plasma concentrations in Sprague-Dawley rats. Results are presented as the mean ± SD, n=3.

Figure 8. MGS0028 and metabolite (MGS0034) plasma concentrations in Rhesus monkeys. Results are presented as the mean ± SD, n=3.

Figure 9. MGS0028 plasma concentrations in Beagle dogs. Results are expressed as the mean ± SD, n=3. The metabolite MGS0034 was not detected in dog plasma.

Figure 10. Allometric scaling to predict human clearance, using three methods from Obach, et al., 1997. C3b: excluding interspecies f_u , including MLP, C3c: including interspecies f_u , excluding MLP, and C3d: excluding interspecies f_u and MLP; where f_u is the unbound fraction of drug in tissues and MLP is maximum lifespan potential. Key: The circles represent data points for Log(BW) vs. Log(Cl_p). The straight line is the plot of the predicted line from linear regression. The triangle is the calculated prediction for human clearance.

DMD #4978

Table 1. Pharmacokinetic parameters derived from total radioactivity following single dose administration of [¹⁴C]MGS0028 to Sprague-Dawley rats. [¹⁴C]MGS0028 was dissolved in isotonic saline containing 0.3% Tween 80 for both IV and PO administration. The radiolabel doses and dosing volumes were 3.7 MBq/mL/kg for IV administration and 1.8-3.7 MBq/5mL/kg for PO administration.

Parameter	1 mg/kg IV Rat	1 mg/kg PO Rat	1 mg/kg PO Rat
		(Fasted)	(Fed)
C _{max} (μM)	5.91 ± 1.84	1.15 ± 0.26	0.49 ± 0.02
T _{max} (hr)	--	0.8 ± 0.2	1.7 ± 0.3
AUC _{0-24hr} (μM*hr)	5.94 ± 1.26	3.40 ± 0.23	3.63 ± 0.39
F (%)	--	57	61
T _{1/2} (hr)	2.4 ± 0.6	2.2 ± 0.2	4.8 ± 1.7

Results are presented as mean (± SD), n=3.

-- Not Applicable.

DMD #4978

Table 2. Cumulative excretion of radioactivity (% dose) from a 1 mg/kg dose of [¹⁴C]MGS0028 to Sprague-Dawley rats. [¹⁴C]MGS0028 was dissolved in isotonic saline containing 0.3% Tween 80 for both IV and PO administration. The radiolabel doses and dosing volumes were 3.7 MBq/mL/kg for IV administration and 1.8-3.7 MBq/5mL/kg for PO administration.

Time (hr)	IV			PO		
	Urine	Feces	Total	Urine	Feces	Total
0-8	73.1 ± 1.8	--	73.1 ± 1.8	65.6 ± 1.9	--	65.6 ± 1.9
0-24	88.7 ± 2.8	2.2 ± 0.4	90.9 ± 2.5	90.4 ± 1.5	3.0 ± 0.0	93.4 ± 1.5
0-48	90.3 ± 2.7	4.3 ± 1.9	94.6 ± 1.2	92.5 ± 1.4	3.7 ± 0.1	96.2 ± 1.4
0-72	90.8 ± 2.7	4.7 ± 2.1	95.5 ± 1.1	93.0 ± 1.4	3.9 ± 0.1	96.9 ± 1.4

Results are presented as mean (± SD), n=3.

-- Not Available. Feces collected in 24 hr intervals only.

DMD #4978

Table 3. Pharmacokinetic parameters of MGS0028 in Sprague-Dawley rats, Rhesus monkeys, and Beagle dogs.

Dose	Sprague-Dawley Rat				Rhesus Monkey		Beagle Dog		
	3 mg/kg IV	1 mg/kg PO	3 mg/kg PO	10 mg/kg PO	1 mg/kg IV	5 mg/kg PO	0.3 mg/kg IV	0.1 mg/kg PO	0.3 mg/kg PO
C_{max} (μM)	--	1.0 ± 0.2	2.7 ± 0.3	6.0 ± 1.9	--	1.0 ± 0.5	--	1.5 ± 0.8	4.0 ± 1.0
T_{max} (hr)	--	0.8 ± 0.2	2.0 ± 0.0	3.0 ± 1.4	--	2.3 ± 1.5	--	0.4 ± 0.1	0.5 ± 0.0
AUC_{0-24hr} (μM*hr)	14.3 ± 0.8	3.4 ± 0.5	9.7 ± 1.2	35.8 ± 3.8	10.2 ± 2.6	10.4 ± 5.0	8.2 ± 1.1	1.7 ± 0.9	5.7 ± 0.3
Effective T_{1/2} (hr)	1.1	--	--	--	1.1	--	0.9	--	--
CL_p (mL/min/kg)	16.2 ± 0.9	--	--	--	8.0 ± 1.8	--	2.8 ± 0.4	--	--
Vd (L/kg)	0.5 ± 0.2	--	--	--	0.6 ± 0.1	--	0.1 ± 0.01	--	--
F (%)	--	70.7	67.7	75.3	--	20.3*	--	63.4	69
AUC_{Metabolite}/AUC_{Parent}	0.8	0.4	0.6	0.3	0.3	0.9	0.0	0.0	0.0

Results are presented as mean (± SD), n=3, except for dog at 0.1 mg/kg PO, where n=2.

-- Not Applicable. *Some monkeys experienced emesis and this may be partially responsible for low bio-availability.

DMD #4978

Table 4. Protein binding of [¹⁴C]MGS0028 in rat, dog, monkey and human plasma was determined using an ultracentrifugation method. Plasma was spiked with [¹⁴C]MGS0028 at concentrations of 1 and 10 μM (840 - 8400 Bq).

Unbound Fraction in Plasma, %				
Concentration (μM)	Rat	Dog	Monkey	Human
10	71.5 ± 1.2	72.1 ± 0.8	71.0 ± 2.2	67.9 ± 2.1
1	71.9 ± 1.0	71.7 ± 2.5	72.7 ± 1.6	68.5 ± 2.3

Results are mean ± SD, n=3.

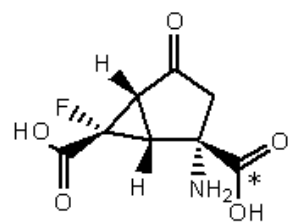
DMD #4978

Table 5. Predicted human pharmacokinetic parameters.

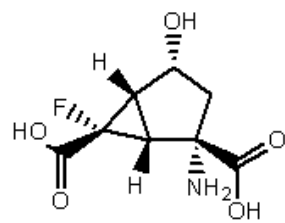
	Vd		Cl
V2	0.1	C3b	4.02
V3a	0.08	C3c	2.1
V3b	0.11	C3d	1.51
Ave Vd	0.09	Calculated	1.04

Methods reported by Obach, et al., 1997.

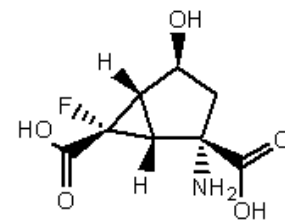
Figure 1



[14C]MGS0028



MGS0034



MGS0025

Figure 2

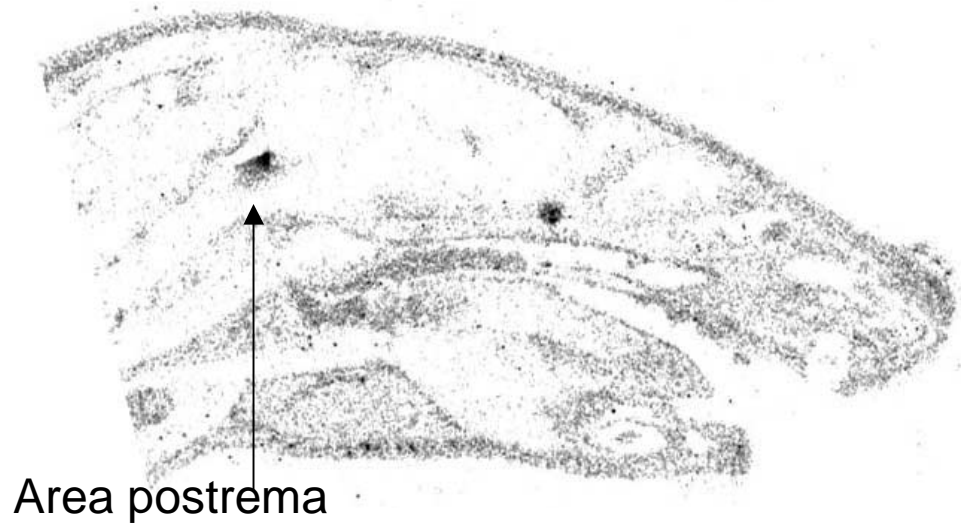


Figure 3

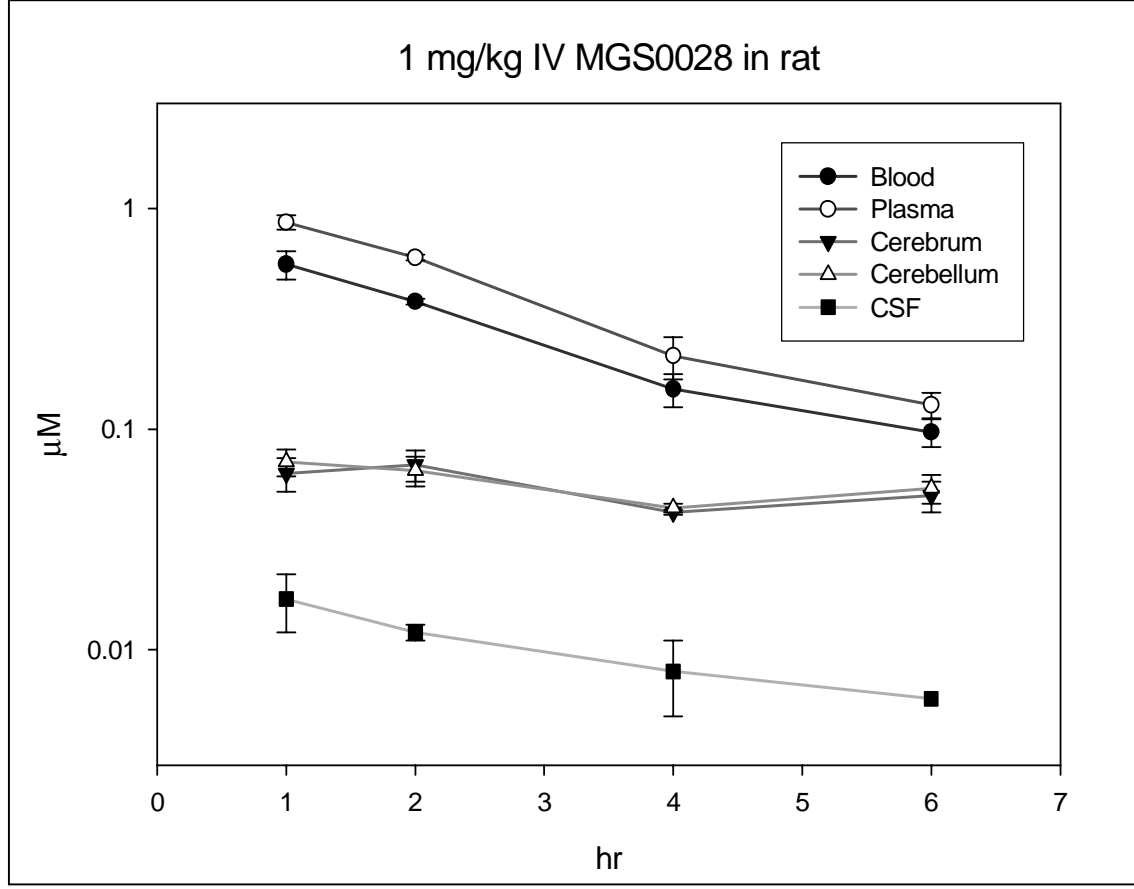


Figure 4

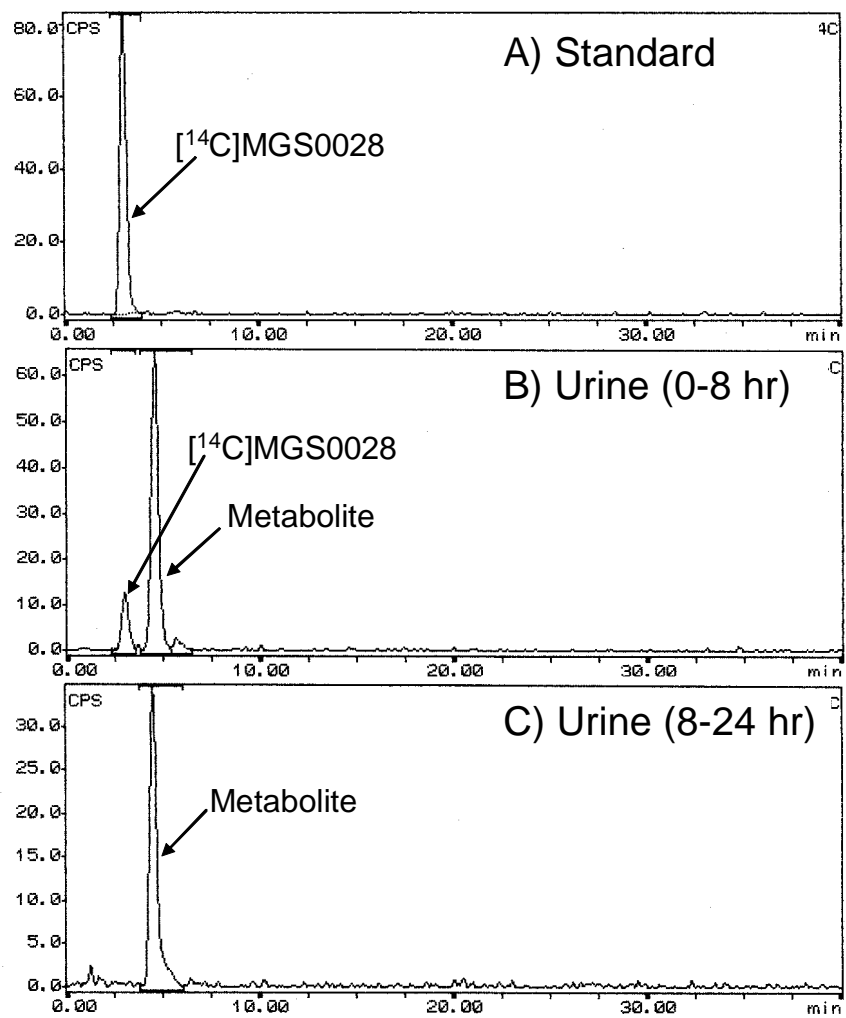


Figure 5

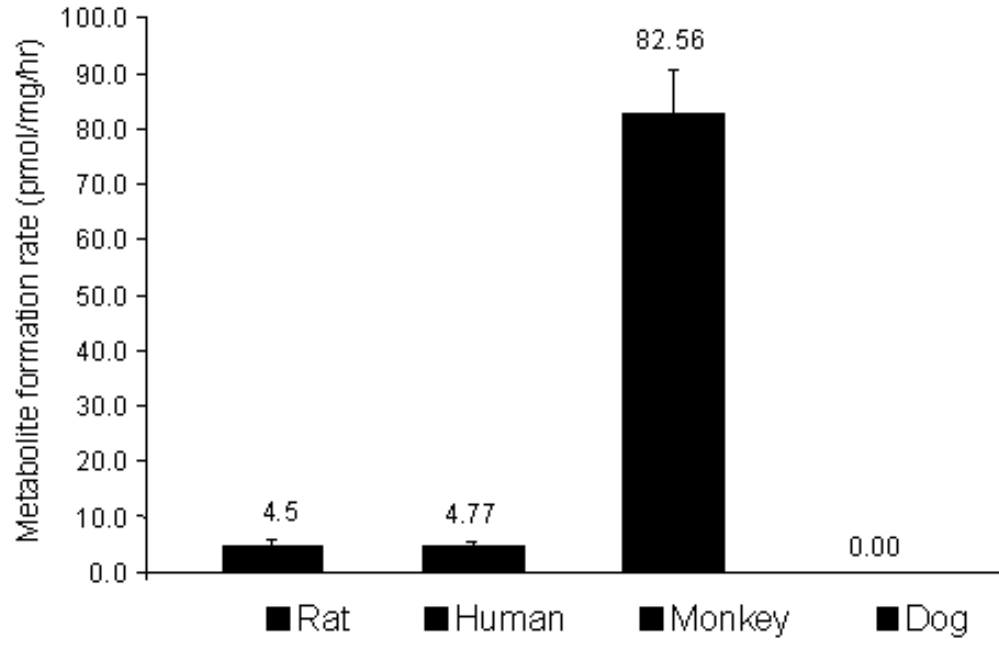


Figure 6

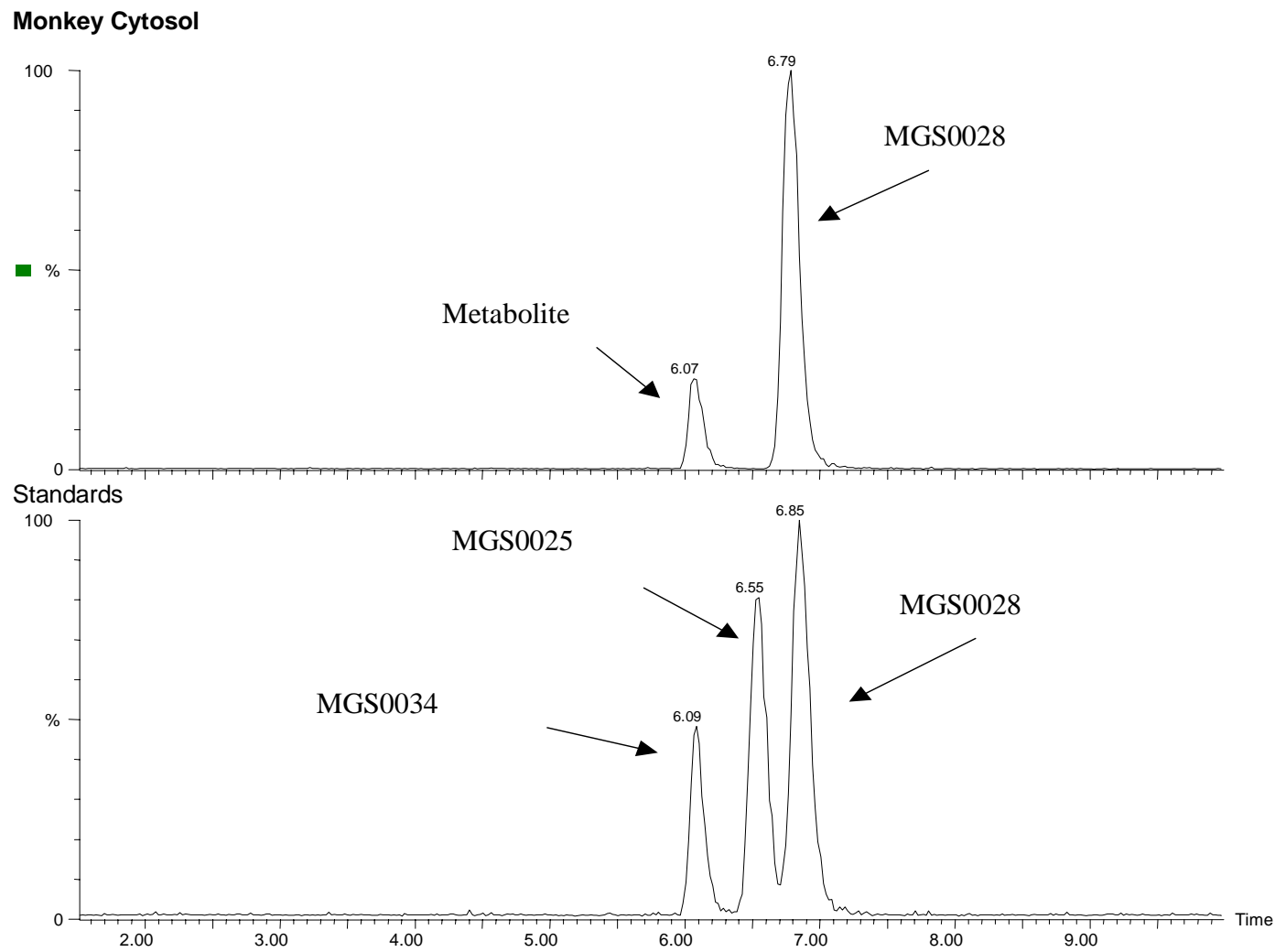


Figure 7

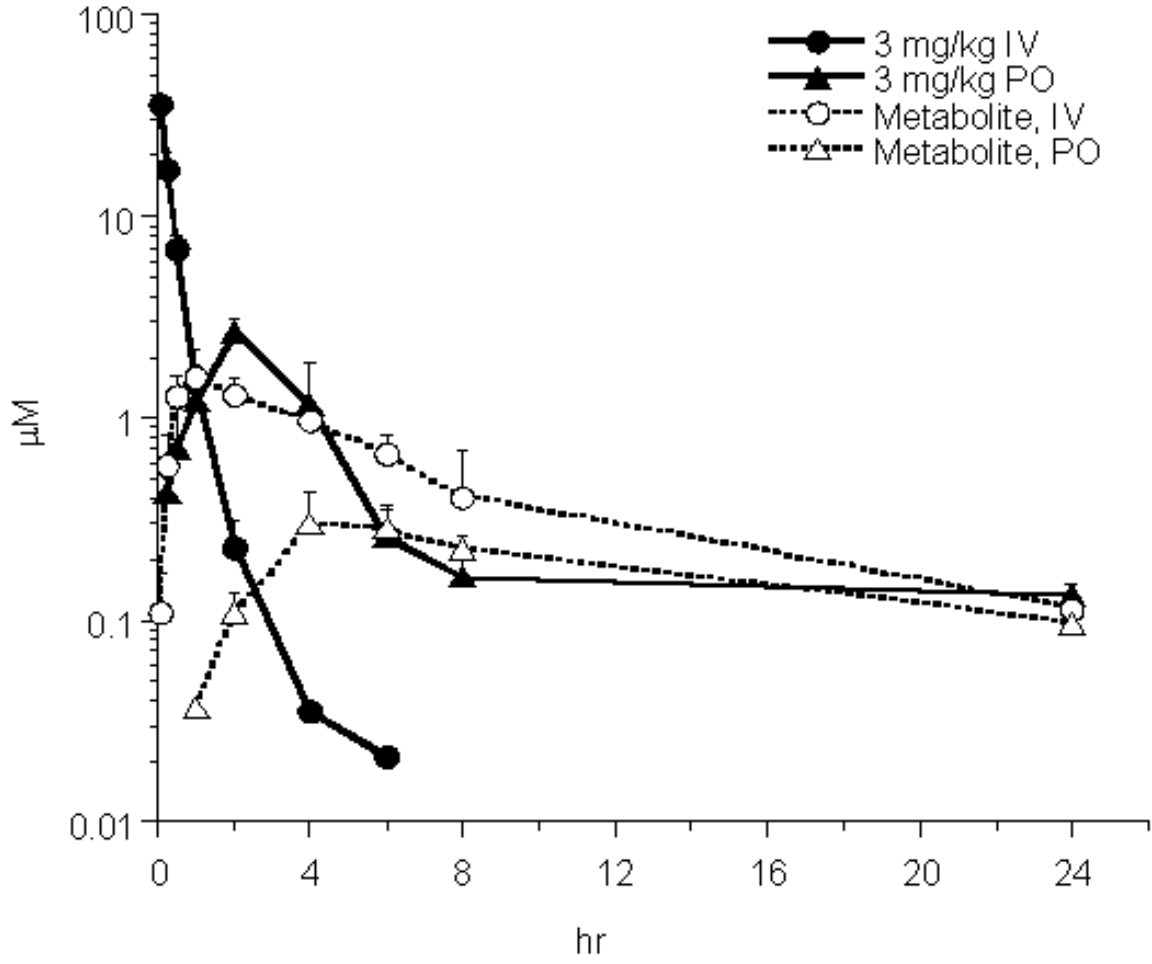


Figure 8

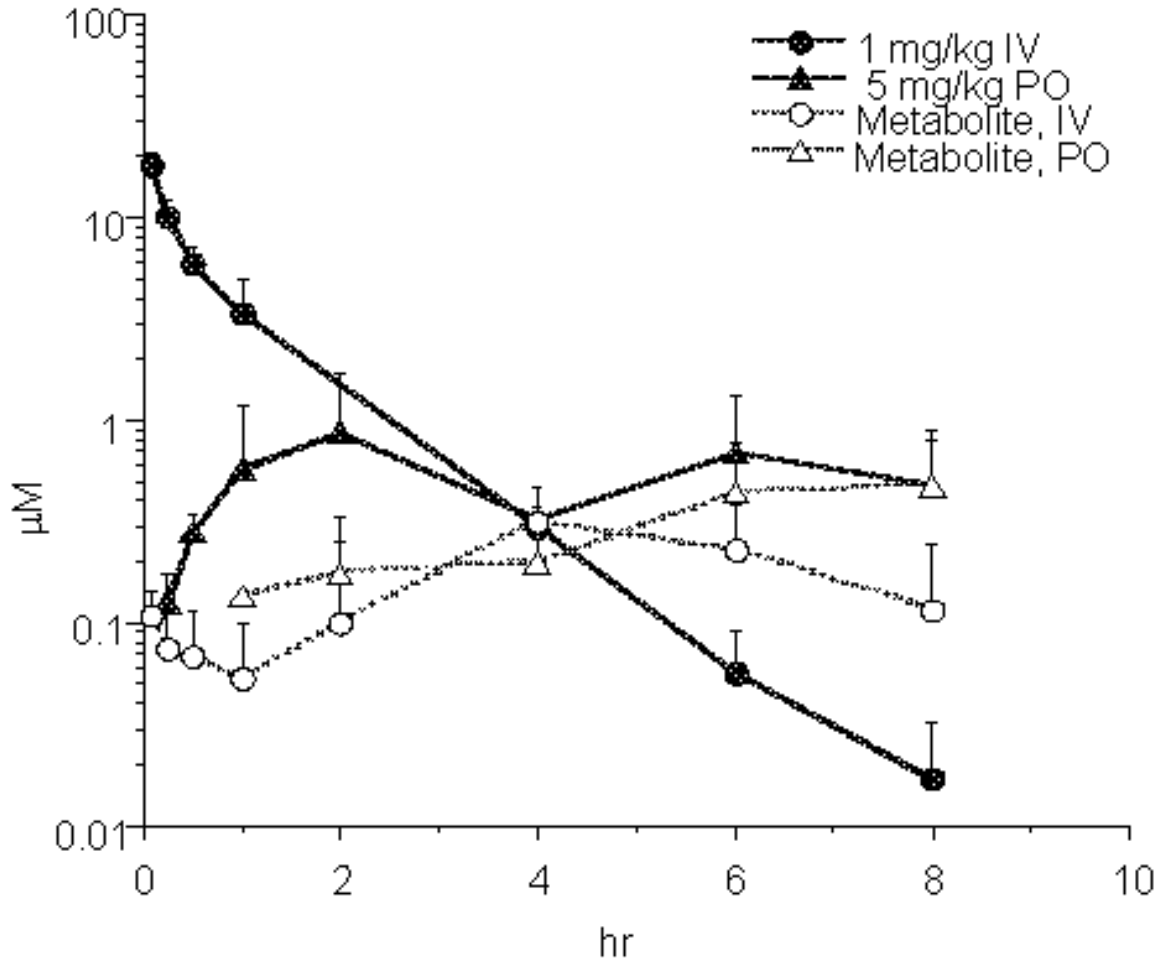


Figure 9

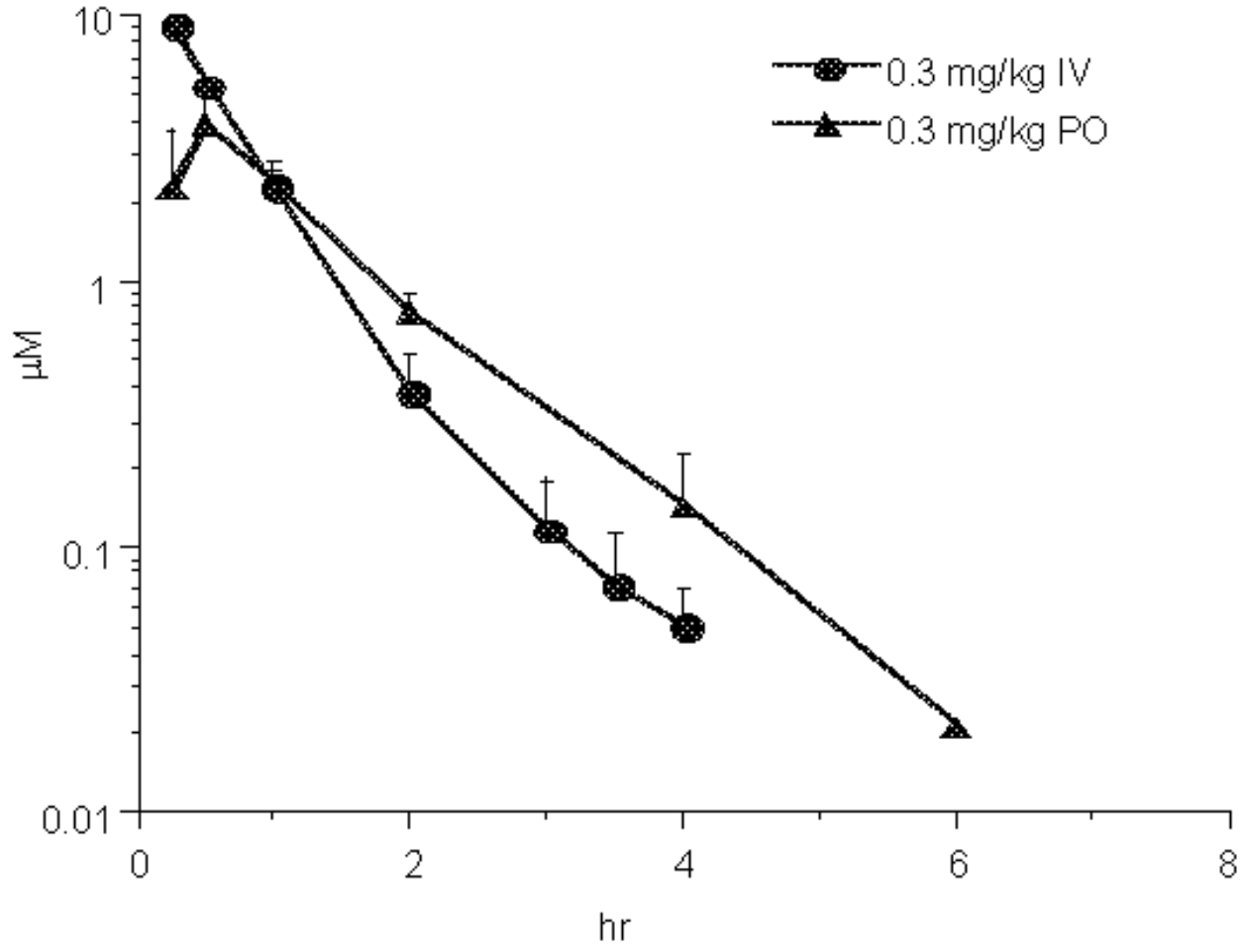
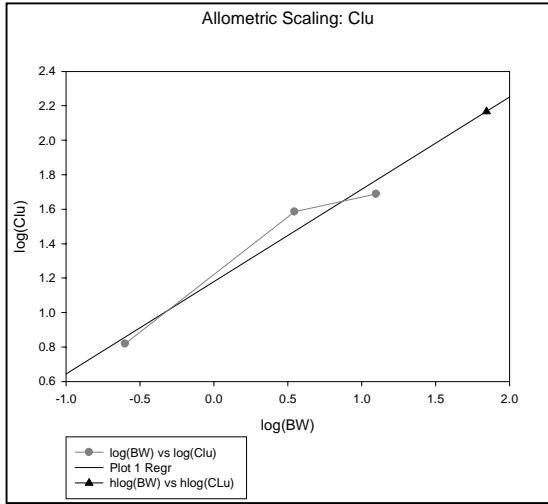
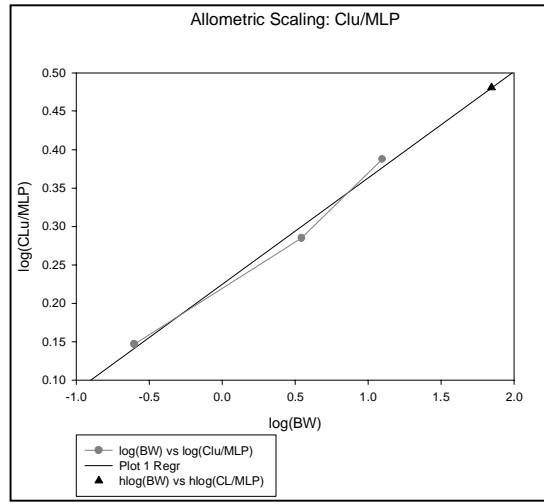


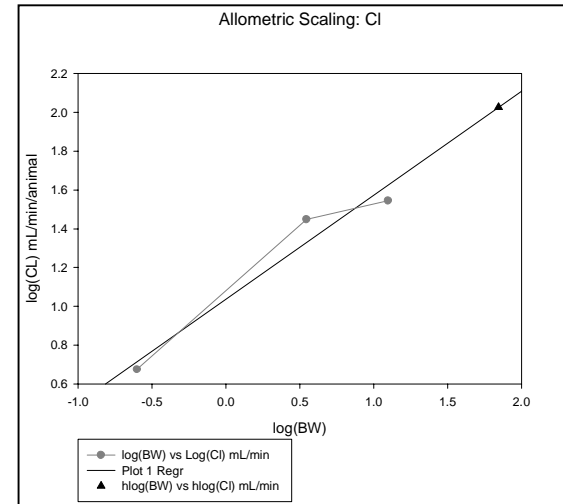
Figure 10



Method C3b



C3c



C3d